J. Am. Soc. Mass Spectrom. (2018) 29:1678–1687
DOI: 10.1007/s13361-018-1991-1

RESEARCH ARTICLE

Atmospheric Solid Analysis Probe Coupled to Ion Mobility Spectrometry-Mass Spectrometry, a Fast and Simple Method for Polyalphaolefin Characterization

Anna Luiza Mendes Siqueira,[1,2] Mathieu Beaumesnil,[1,2] Marie Hubert-Roux,[1] Corinne Loutelier-Bourhis,[1] Carlos Afonso,[1] Yang Bai,[2] Marion Courtiade,[2] Amandine Racaud[2]

[1]Normandie Univ, COBRA, UMR6014 and FR3038, Université de Rouen, INSA de Rouen, CNRS, IRCOF, 1 rue Tesnière, 76821, Mont-Saint-Aignan Cedex, France
[2]TOTAL Marketing Services, Research Center, 69360, Solaize, France

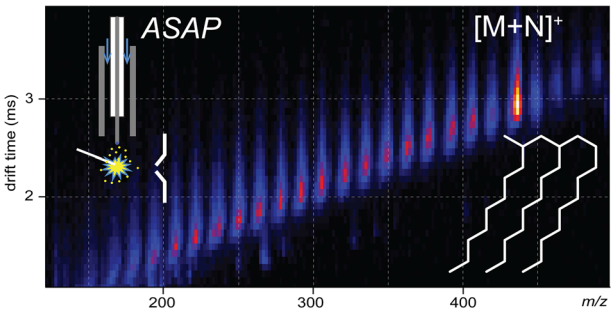

Abstract. Polyalphaolefins (PAOs) are polymers produced from linear alpha olefins through catalytic oligomerization processes. The PAOs are known as synthetic high-performance base stock fluids used to improve the efficiency of many other synthetic products. In this study, we report the direct characterization of PAOs using atmospheric solid analysis probe (ASAP) coupled with ion mobility spectrometry-mass spectrometry (IMS-MS). We studied different PAOs grades exhibiting low- and high-viscosity index. Specific adjustments of the ASAP source parameters permitted the monitoring of ionization processes as three mechanisms could occur for these compounds: hydride abstraction, nitrogen addition, and/or the formation of $[M–2H]^{+\bullet}$ ions. Several series of fragment ions were obtained, which allowed the identification of the alpha olefin used to synthesize the PAO. The use of the ion mobility separation dimension provides information on isomeric species. In addition, the drift time versus *m/z* plots permitted rapid comparison between PAO samples and to evidence their complexity. These 2D plots appear as fingerprints of PAO samples. To conclude, the resort to ASAP-IMS-MS provides a rapid characterization of the PAO samples in a direct analysis approach, without any sample preparation.

Keywords: ASAP-IMS/MS, Polyalphaolefin characterization, Synthetic fluids, Pyrolysis

Received: 30 March 2018/Revised: 4 May 2018/Accepted: 8 May 2018/Published Online: 31 May 2018

Introduction

Demands of high-performance synthetic fluids, such as polyalphaolefins (PAOs), continue to grow over the years, as an alternative to decrease the consummation of petroleum resources and to improve the functional fluid characteristics based on mineral oils [1]. PAOs are saturated alpha olefin oligomers used as base stock oil for synthetic lubricants. Due to their exclusive chemical and physical properties, the PAOs are widely employed for automotive and industrial applications [2].

The synthetic base stocks are manufactured by catalytic oligomerization of linear alphaolefins, usually C_{10}. However, C_6, C_8, C_{12}, and C_{14} alphaolefins, pure or in mixtures, can also be used to synthesize PAOs. The more conventional catalytic methods are either Ziegler-Natta [3, 4] or Friedel-Crafts catalysis [2, 4]. Other oligomerization pathways have been developed, and free radical oligomerization [5], metallocene catalysis [6, 7], the use of ionic liquids [8], and synthetic zeolites [9]

Electronic supplementary material The online version of this article (https://doi.org/10.1007/s13361-018-1991-1) contains supplementary material, which is available to authorized users.

Correspondence to: Corinne Loutelier–Bourhis;
e-mail: corinne.loutelier@univ–rouen.fr, Carlos Afonso;
e-mail: carlos.afonso@univ–rouen.fr

have also been used to produce PAOs. The choice of the oligomerization process leads to the development of a particular type of PAO and permits to control the final product properties and characteristics, such as viscosity and degree of branching [3, 4, 10, 11]. The processes involved in the PAO production are given in Figure 1. After oligomerization, the unsaturated products (dimers, trimers, tetramers, and others) are converted through a hydrogenation process using a supported metal catalyst with nickel or palladium, resulting in a mixture of branched, acyclic, and saturated alkanes with different molecular weights. Then, a distillation process allows the separation of PAOs contained in the mixture into different grades and the elimination of unreacted alpha olefins. The PAOs can be classified in grades according their kinematic viscosity at 100 °C [12, 13].

The outstanding chemical and physical properties exhibited by PAOs, when compared to mineral oils, are high-viscosity index, lower-temperature fluidity, greater thermal and oxidative stability, lower volatility, higher flash point, and low toxicity. These characteristics make them attractive fluids to improve the quality of greases, gels, and various oils used in transmission and hydraulic fluids in blends, for compressor and turbine [2, 12].

To allow a better understanding of the PAO structure and their performance, the analysis of different synthetic base oils is necessary. The characterization of PAOs was previously reported in the literature using nuclear magnetic resonance (NMR) [14, 15] and gas chromatography coupled to mass spectrometry (GC-MS) techniques [2, 16, 17]. However, only low PAO grades synthesized from 1-decene were analyzed using those techniques as high molecular weight hydrocarbons could not be eluted using GC methods [14, 16, 18].

Recently, some analyses of non-volatile materials have been reported using a new source device named atmospheric solid analysis probe (ASAP) that appeared to be a good alternative for rapid analysis of solid or liquid samples [19–23]. Indeed, this source can permit a direct analysis without sample preparation. Introduced by McEwen in 2005, the ASAP source was firstly used to analyze volatile and semi-volatile compounds present in biological tissues and polymeric materials [19]. The ASAP probe consists in a glass capillary tube in which the sample is directly deposited. A nitrogen gas flow, which can be heated from 50 °C to the maximum probe temperature (650 °C), is used to thermally desorb the sample. Once in the gas phase, the sample is ionized by nitrogen plasma generated by a corona discharge [20]. This technique permitted to characterize a wide range of complex materials, such as biological fluids [24], drugs [25], pesticides [26], polymers [21, 27–30], lubricants [22], coal [31], or crude oil [32–34].

Moreover, the coupling of ASAP with ion mobility spectrometry-mass spectrometry (IMS-MS) has been reported as an efficient approach for the characterization of complex samples [21, 22], in particular, as IM adds an extra dimension of separation to MS [21, 22, 33, 35, 36]. In IM, the analysis is based on the movement of ions in an ion mobility cell through a buffer gas and in the presence of an electric field. The ions are separated according to their size, charge, and shape [37, 38].

In this work, we proposed to use ASAP to provide a direct and fast characterization of any grade of PAO, without sample preparation. Then, the ASAP-IMS-MS coupling was considered an efficient and original approach to analyze synthetic base oils of different viscosity grades and synthesized from different alpha olefin monomers.

Experimental

Sample Preparation

All polyalphaolefin samples were supplied by Total Research Center (Solaize, France). The PAO samples were analyzed without sample preparation (Table 1).

Ion Mobility-Mass Spectrometry

A hybrid quadripole ion mobility-time of flight mass spectrometer (Synapt G2, Waters Corp., Manchester, UK) fitted with an ASAP source was used to perform the analyses. This instrument presents three successive traveling wave-enabled stacked ring ion guides: the trap, the IMS, and the transfer cells. The instrument has been described in detail elsewhere [39, 40]. Prior to sample introduction, the ASAP glass capillary fitted into the ASAP probe was baked in the ion source at 650 °C for 2 min to avoid any residual contamination that may be present in the capillary surface. A blank spectrum was recorded during 1 min. Then, the ASAP capillary was dipped into the sample and then introduced into the source. The ASAP source was operated in positive mode, over the *m/z* 50–2000 range, in V resolution mode. The corona discharge was set at 20 μA, the extraction cone was 5 V, the nitrogen gas flow was 1200 L/h, and the source temperature was 140 °C. For the analyses of low and high PAO grades, sample cone and desolvation gas temperature were optimized as follows: the sampling cone voltage was varied from 20 to 80 V and the desolvation gas temperature was increased from 200 to 650 °C in 100 °C increments each

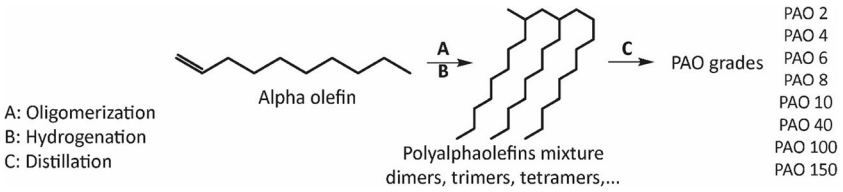

Figure 1. Different steps used to manufacture the PAOs

Table 1. Information About the PAOs Analyzed by ASAP-IMS-MS

Name	Grade	Type of catalysis	Alphaolefin used for synthesis
PAO-A	3.6	Lewis acid	C10
PAO-B	3.6	Lewis acid	C10
PAO-C	3.6	Lewis acid	C10
PAO-D	150	Lewis acid	C10
PAO-E	150	Metallocene	C8
PAO-F	150	Metallocene	Mixture
PAO-G	100	Lewis acid	Mixture

minute. In the ASAP-MS/MS experiments, the precursor ions were selected using the quadrupole and were collisionally activated in the trap cell, and various collision energies were tested; 5, 10, and 30 eV and argon was used as the collision gas. The IMS-MS conditions were set as follows:

- For data presented in Figure 4: IMS nitrogen gas flow, 90 mL/min; helium cell, 180 mL/min; traveling wave height, 40 V; and velocity traveling wave, 1000 m/s.
- For data presented in Figures 7 and 8: IMS nitrogen gas flow, 50 mL/min; helium cell, 150 mL/min; traveling wave height, 40 V; and velocity traveling wave, 700 m/s.

Data were acquired during 5 min over a range of *m/z* 50–2000. Before the analyses, the mass spectrometer was externally calibrated with sodium formate solution (2 mg/mL) and using an electrospray source. Note that *m/z* 277.0782 which corresponds to a background ion of the ASAP source (fragment ion of phenylphosphine oxide present as a flame retardant), as previously described [21], was used as internal standard for accurate mass measurement. Data acquisition and mass spectra were performed using MassLynx (version 4.1) software. DriftScope (version 2.2) was used to the treatment of ion mobility data. Ion mobility peaks were fitted using OriginPro (version 9.1) software.

Results

Low Viscosity Grade PAOs

Influence of Source Parameters on the Ionization of Low-Grade PAOs Among the ASAP source parameters, we found that the sampling cone voltage and the desolvation gas temperature had a crucial influence on the resulting mass spectra. Adjusting the sampling cone voltage allowed (i) to maximize ion signal of intact species by minimizing in-source fragmentation and (ii) the monitoring of ionization processes. Another key instrumental parameter of the ASAP source was the desorption temperature. The resort of a temperature gradient provides a gradual desorption of the compounds according to their volatility and boiling point. The gradient helps to determine the temperature range for optimal desorption while avoiding thermal fragmentation and pyrolysis.

Figure 2 depicts ASAP mass spectra of PAO-A grade 3.6 recorded at different sampling cone values and using a temperature gradient. The PAO-A is synthesized from decene and mainly corresponds to C30 oligomers. At low sampling cone

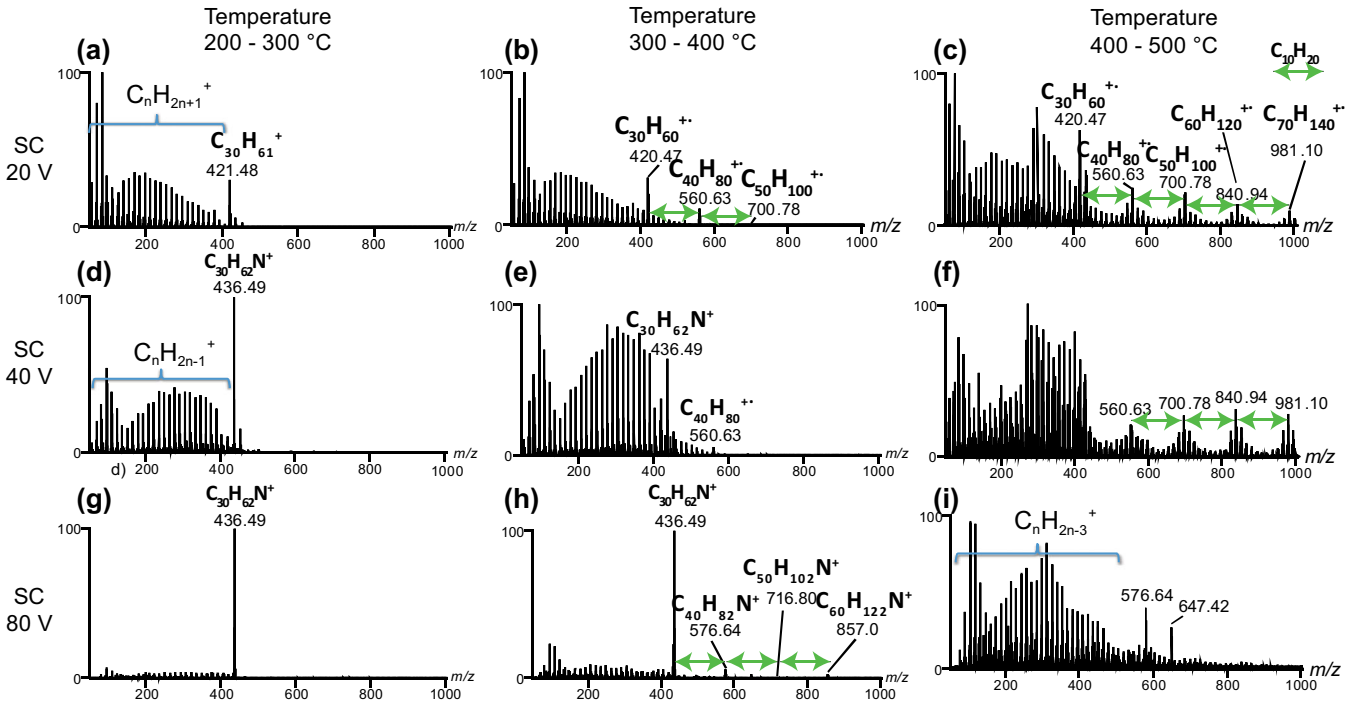

Figure 2. ASAP-MS spectra of PAO A (grade 3.6) containing mainly C30 oligomers recorded at different ranges of temperature (200 to 500 °C) and sampling cone (SC) voltages (20, 40, and 80 V)

voltage (20 V) and temperature gradient 200 to 300 °C, the mass spectrum showed a distribution of $C_nH_{2n-1}^+$ ions and a distinct *m/z* 421.47 which corresponds to $[M-H]^+$ of the C30 oligomer ($C_{30}H_{61}^+$, measured/calculated *m/z* values 421.4766/421.4768) (Figure 2a). The $[M-H]^+$ species results most likely from a hydride abstraction process, well described in the literature as ionization pathway for non-polar compounds [32, 41, 42]. The series of $C_nH_{2n-1}^+$ ions (14.02 *m/z* units shift) could arise from competitive thermal fragmentation of C30 oligomer: either from unspecific losses of alkene molecules from the carbenium $[M-H]^+$ ion ($C_{30}H_{61}^+$) or from unspecific σ-bond C–C of $M^{+\bullet}$ ion by free radical processes. We cannot exclude the hypothesis that the $M^{+\bullet}$ ion can be formed in the source but is promptly fragmented because too unstable.

When we increased the desolvation gas temperature (Figure 2b), the detection of unexpected $[M-2H]^{+\bullet}$ species was promoted: *m/z* 420.46, *m/z* 560.62, and *m/z* 700.78 (in a lesser extent) were detected and corresponded to $C_{30}H_{60}^{+\bullet}$, $C_{40}H_{80}^{+\bullet}$, and $C_{50}H_{100}^{+\bullet}$, respectively. The measured/calculated *m/z* values for these species were found to be 420.4685/420.4690, 560.6257/560.6255, and 700.7805/700.7820. We can assume that the increase of the temperature favored the formation of radical cations that have eliminated H_2 neutral loss. Moreover, the increase of the temperature also permitted the desorption of higher molecular weight ions. Note that these three ions are separated by 140.16 *m/z* units which correspond to a repeating unit of $C_{10}H_{20}$. This was expected since PAO-A was synthetized by 1-decene oligomerization. Thus, ASAP-MS spectra provide information about the repeating unit of the synthesized PAO from 1-decene.

The $[M-2H]^{+\bullet}$ ions can be explained by H_2 loss from the molecular ions [43, 44] as the formation of such ions had previously been reported for saturated hydrocarbons using atmospheric pressure chemical ionization (APCI) [45] and field desorption (FD) [46]. These studies showed that the ionization of highly branched alkanes such as squalane and 2,6,10,14-tetramethylpentadecane can produce $[M-2H]^{+\bullet}$ ions. Thus, the detection of $[M-2H]^{+\bullet}$ ions is consistent with the highly branched character of the PAO-A synthetic base oil.

When the desorption temperature was further increased beyond 400 to 500 °C (Figure 2c), $[M-H]^+$ and $[M-2H]^{+\bullet}$ ions of higher molecular weight such as C60 and C70 oligomers were observed, but as low-abundant species. The use of temperature gradient using high temperature helps the detection of higher MW oligomers, present in small amounts in the sample.

When the sampling cone voltage was increased up to 40 V (Figure 2d), the mechanism of nitrogen insertion was observed: the *m/z* 436.48 corresponded to $C_{30}H_{62}N^+$ ion (measured/calculated *m/z* 436.4879/436.4877). This phenomenon was firstly reported by Cooks et al. [47] when they analyzed saturated hydrocarbons by FD-MS. Then, Wu and co-workers [32] observed the nitrogen fixation in aliphatic and aromatic hydrocarbon standards, but also in petroleum-saturated hydrocarbon fractions, using the ASAP source. For high-temperature ranges (Figure 2e, f), the pyrolysis of polyalphaolefin becomes the main process: the intensities of the resulting fragment ions increase.

The nitrogen addition becomes the predominant ionization process for higher sampling cone voltage (80 V); thus, the $C_{30}H_{62}N^+$ ion is the main species in Figure 2g. However, the increase of higher sampling cone voltage induces fragmentation: two distinct distributions of fragment ions were detected in Figure 2g. The major distribution corresponds to $C_nH_{2n-2}N^+$ ions and the less intense distribution corresponds to $C_nH_{2n}N^+$ ions. The nitrogen insertion was also observed for C40, C50, and C60 oligomers (measured/calculated *m/z* values 576.6409/576.6442, 716.8024/716.8007, and 856.9540/856.9572, respectively) when temperature increased (Figure 2h).

The fragmentation of the PAO-A was predominant in Figure 2i, where high-abundant C_nH_{2n-3} species were detected. The detection of C30 oligomer was no more achieved at sampling cone 80 V and temperature between 400 and 500 °C, meaning that these sampling cone voltage and temperature conditions were no more suitable for C30 polyalphaolefin. However, the nitrogen insertion was mostly observed for C40 oligomer. Note that the additional ion detected at *m/z* 647.42 could be attributed to an impurity present in the sample.

MS/MS of PAO-A Ions The product ion spectrum of $[M-2H]^{+\bullet}$ *m/z* 420.47 ($C_{30}H_{60}^{+\bullet}$) is depicted in Figure 3a. The collision energy was set at 10 eV. This ion corresponds formally to an alkene molecular ion. Its fragmentation produced a major alkenyl series $C_nH_{2n-1}^+$ and a less-abundant $C_nH_{2n}^{+\bullet}$ ion series through the losses of alkane and alkyl radical, respectively. These series correspond to those currently observed for EI-MS analysis of alkenes [48].

The product ion spectrum of *m/z* 421.48 was acquired collision energy at 5 eV. The fragmentation of the $[M-H]^+$ ($C_{30}H_{61}^+$) ion, formed from hydride abstraction, led to the series of carbenium ion fragments ($C_nH_{2n+1}^+$) which are usually encountered in CI-MS of alkanes [49–52] (Figure 3b).

The product ion spectrum of *m/z* 436.49 $[M+N]^+$ was acquired using a collision energy of 30 eV, showing that this ion is significantly more stable that the $[M-2H]^{+\bullet}$ and $[M-H]^+$. The fragmentation of the $C_{30}H_{62}N^+$ ion leads to the formation of the iminium ion distribution (Figure 3c), previously described by Cooks et al. for saturated hydrocarbons [47]. Such distribution arises by elimination of alkenes from the precursor ion. The formation of alkenyl ions (*m/z* 55.07, *m/z* 69.07, *m/z* 97.10, and *m/z* 111.12) and carbenium ions (*m/z* 57.07, *m/z* 71.09, and *m/z* 85.10) are also observed. The high stability of the $[M+N]^+$ explains why the remaining ions in the mass spectra are recorded with high sampling cone values (Figure 2g, h).

IMS-MS Analysis With the IMS-MS coupling, information about conformation of the ions in gas phase can be obtained. The three PAOs (PAO-A, PAO-B, and PAO-C) presenting the same grade (3.6) and synthesized using Lewis acids were studied using ASAP-IMS-MS. The PAO grades 3.6 were

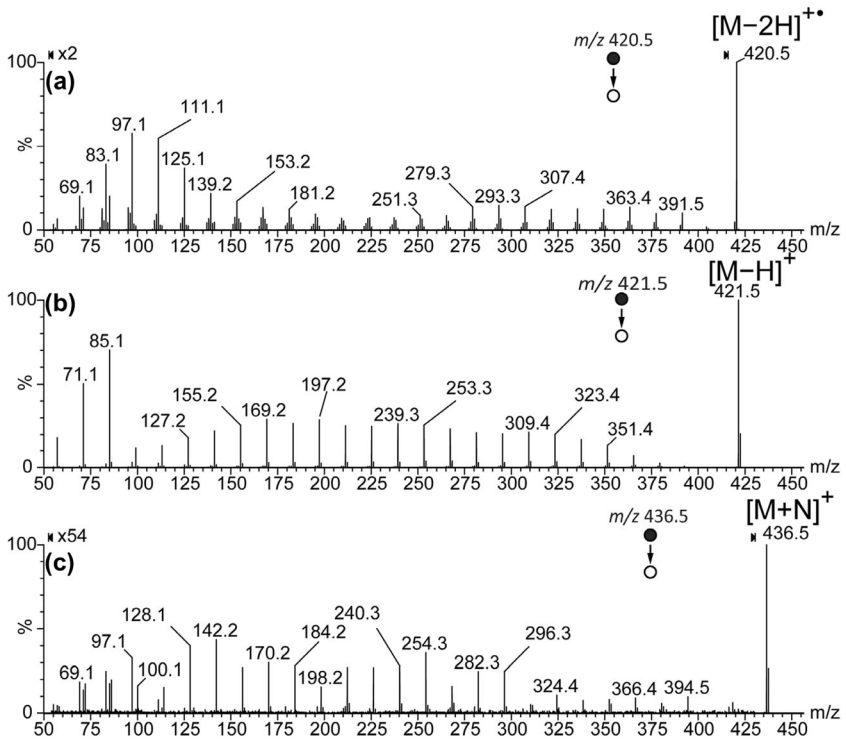

Figure 3. MS/MS spectra of (**a**) *m/z* 420.47 ion using collision energy at 10 eV, (**b**) of *m/z* 421.48 ion using collision energy at 5 eV, and (**c**) of *m/z* 436.49 ion using collision energy at 30 eV

synthesized from 1-decene, so C30 oligomers are expected to be obtained. Thus, these three PAOs are mainly constituted by C30 oligomers, and these results were confirmed by GC × GC-FID analysis (Table S1). Figure 4 shows the extracted ion mobility spectra for the *m/z* 420.47, which corresponds to $[M-2H]^{+\bullet}$ of the C30 oligomer. Because of the relatively low sampling rate of the ion mobility spectra, a Gaussian peak fit was carried out to accurately determine the peak apex. The drift time of *m/z* 420.47 for PAO-A, PAO-B, and PAO-C was 8.86 ± 0.02, 8.69 ± 0.05, and 8.92 ± 0.01 ms, respectively. This indicates that PAO-B presents, in average, a more compact conformation than PAO-A and PAO-C.

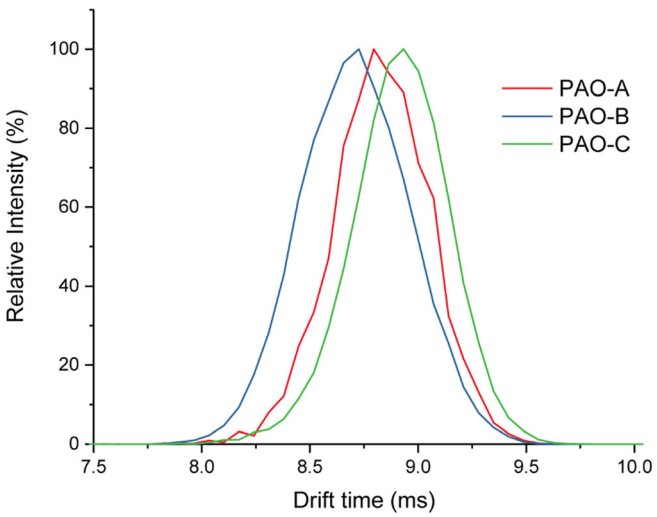

Figure 4. Extracted ion mobility spectra for *m/z* 420.47 for PAO-A (red), PAO-B (blue), and PAO-C (green) grade 3.6

Note that there are no significant differences between the ion mobility peak width obtained for PAO-A and PAO-C (0.52 and 0.53 ms ± 0.01 FWHM, respectively), while the PAO-B signal presents a significantly larger peak width (0.63 ms ± 0.01 FWHM). The error corresponds here to the standard deviation from four experiments. As previously reported, the ion mobility peak width is mainly related to ion diffusion in the drift cell and to the presence of unresolved isomeric species [53]. In the present case, since the *m/z* 420.47 ions of PAO-A, PAO-B, and PAO-C exhibit drift time values of the same order of magnitude (around 8.8 ms), only the presence of a larger number of unresolved isomers can explain the larger peak width for PAO-B (similar ion diffusion being expected in the three cases). Such results were confirmed by GC-MS (Figure S1), which showed that the three PAO samples are complex mixtures of C30 isomers, but the area of unresolved peaks is slightly larger for PAO-B than for PAO-A or for PAO-C. Moreover, the proportions of the different isomers are more diverse for PAO-B than for PAO-A or PAO-C. Note that GC-MS needs more than 30 min for an analysis while IMS-MS only needs few minutes. As previously proposed, the ion mobility peak width can be used as a descriptor for unresolved complex molecular systems and it can allow to differentiate PAOs, which have numerous isomeric structures from those which have no or few ones. Thus, this

indicator should be helpful to correlate the presence of isomers with the properties and performance of synthetic oils.

High Viscosity Grade PAOs

Influence of the Source Parameters on the Ionization of High-Grade PAOs The influence of the sampling cone voltage and the desolvation gas temperature was studied for the ionization of high-viscosity PAO grades. The PAO-D grade 150 was analyzed at different sampling cone voltages (20, 40, and 80 V) and at different temperatures. Figure 5 shows three sets of cone voltage values/temperature values. We also used temperature gradients to follow the progressive desorption of molecules present in the sample. For temperatures between 300 and 400 °C, mainly background ions were detected (data not shown). As expected, higher molecular weight species were desorbed from the glass capillary tube when the temperature increased (Figure 5a versus Figure 5b). Various pyrolysis fragment ions were obtained, and the main species were $C_nH_{2n+1}^+$ and $C_nH_{2n}^{+\bullet}$ ions. We could note that these ions exhibit ion distributions separated by 140.15 u (for example, *m/z* 421.6, *m/z* 561.6, *m/z* 701.8, *m/z* 841.9, and *m/z* 981.9 in case of $C_nH_{2n+1}^+$ ions). This mass shift corresponds to $C_{10}H_{20}$ repeating unit which is specific of the alpha olefin used to produce the PAO, in this case 1-decene. Then, increasing the sampling cone to 40 V (650 °C) improves the transmission of higher masses but also promotes the formation of $C_nH_{2n}^{+\bullet}$ species (Figure 5c). Thus, the distribution of ions from C50 (*m/z* 700.8) to C100 (*m/z* 1401.6) rised up. Again, the mass shift between two adjacent ions permitted to verify that 1-decene was the monomer used to produce the PAO. At sampling cone 80 V, fragmentation processes become so important that only low-mass fragment ions can be detected (data not shown). In the case of high PAO grades, intact species were not observed; only pyrolysis ion distributions were detected. The nitrogen insertion mechanism does not occur for high-viscosity PAOs.

Differentiation of High PAO Grades Three high grade PAOs (PAO-E, PAO-F, and PAO-G) synthesized from two different oligomerization processes, metallocene catalysts (PAO-E and PAO-F, grade 150) and the Lewis acid catalysts (PAO-G, grade 100), were also analyzed by ASAP-IMS-MS. Figure 6 shows the mass spectra acquired from the ASAP-MS experiments for the PAOs. For all PAOs, numerous pyrolysis ions with several

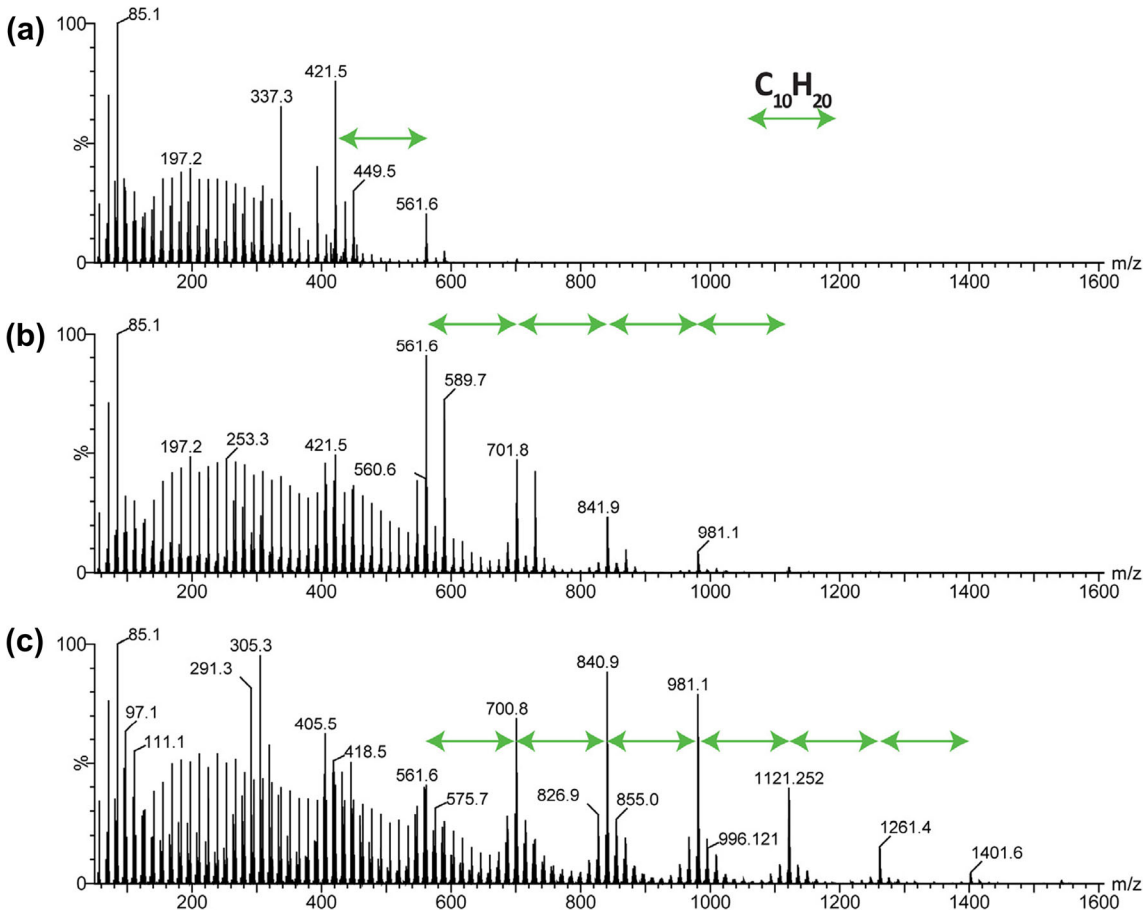

Figure 5. ASAP mass spectra of a high PAO grade (PAO-D, grade 150) at different cone voltage and temperature, sets: (**a**) 20 V/400 to 500 °C range, (**b**) 20 V/650 °C, and (**c**) 40 V/650 °C

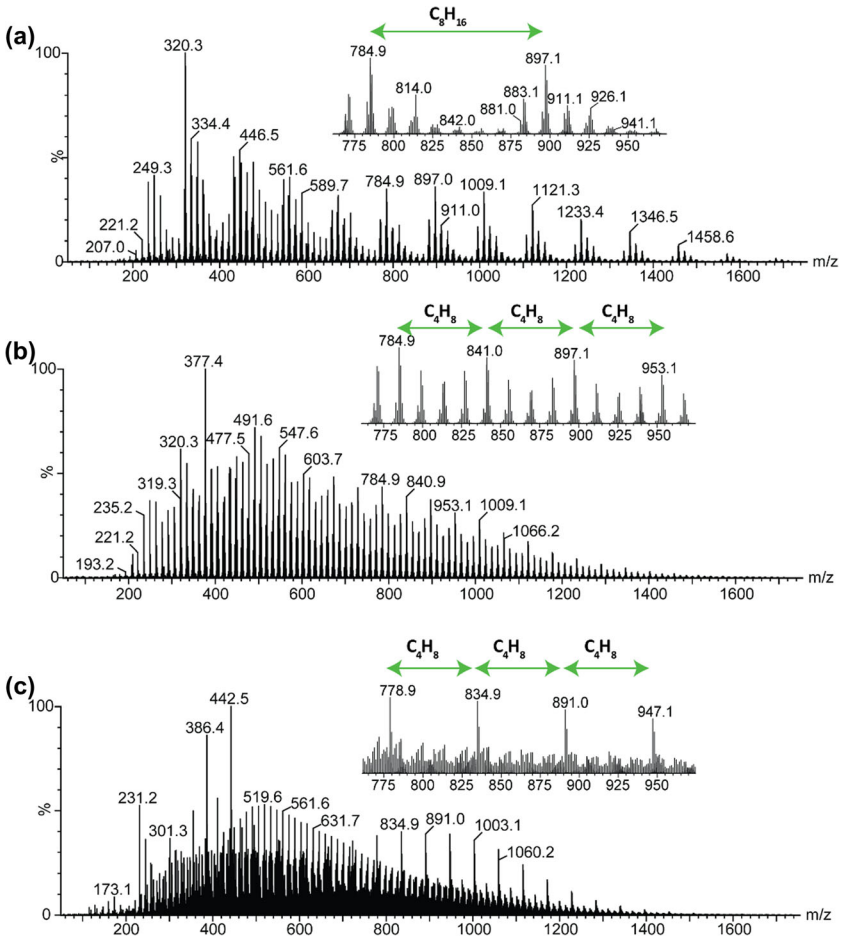

Figure 6. ASAP-MS spectra for (**a**) PAO-E (grade 150), (**b**) PAO-F (grade 150), and (**c**) PAO-G (grade 100), at sampling cone 20 V and temperature at 650 °C

ion series showing a mass shift of 14 *m/z* unit were detected. However, in the case of the PAO-E (grade 150), the major ion distribution exhibits C_8H_{16} repeating unit corresponding to a mass shift of 112.12 u (Figure 6a). This is consistent with a synthesis using 1-octene. In the case of the PAO-F (grade 150), four ion distributions separated by 56.06 u corresponding to C_4H_8 unit were observed (Figure 6b). From these results, it is possible that PAO-F was mainly produced from either 1-butene or a mixture of alphaolefins such as 1-octene and 1-dodecene. However, according to the literature, it is more likely that PAO-F was produced from a mixture of linear C_8 and C_{12} alphaolefins than from 1-butene [2, 4]. For both PAO-E and PAO-F, the $C_nH_{2n+1}^+$ and $C_nH_{2n}^{+\bullet}$ ion series were the most abundant fragment ion series. In the case of PAO-G (grade 100), the mass spectrum is more complex (Figure 6c) and shows higher number of pyrolysis fragment ions, such as $C_nH_{2n+1}^+$, $C_nH_{2n}^{+\bullet}$, $C_nH_{2n-1}^+$ and $C_nH_{2n-2}^{+\bullet}$, $C_nH_{2n-3}^+$, and $C_nH_{2n-4}^{+\bullet}$. These results can be more likely explained by the oligomerization process (Lewis acid catalysis) since it is known that the alphaolefin oligomerization using Lewis acids produces highly branched PAOs [10, 16, 17], which give a higher number of pyrolysis fragment ions during the ASAP analysis. Note that for $m/z > 800$, a main fragment ion series corresponding to $C_nH_{2n-6}^{+\bullet}$ species stands out and exhibits a mass shift of 56.06 *m/z* unit (C_4H_8), meaning that PAO-G can

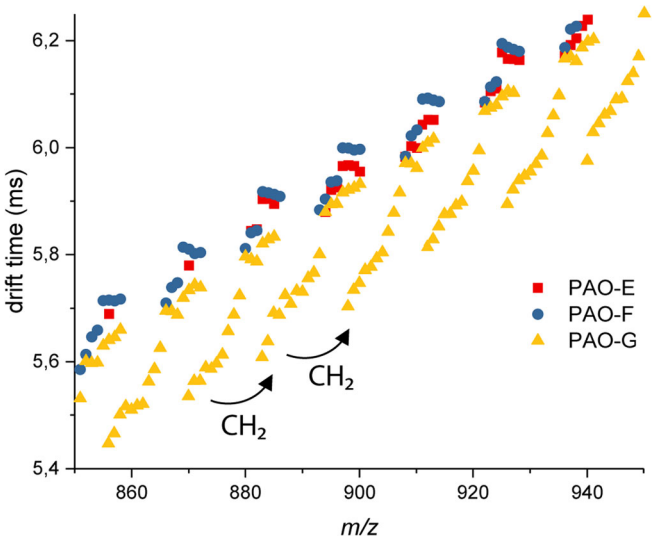

Figure 7. Drift time versus *m/z* plot of PAO-E (red square), PAO-F (blue circle), and PAO-G (yellow triangle) extracted from ASAP-IMS-MS experiments, *m/z* 850–950 range

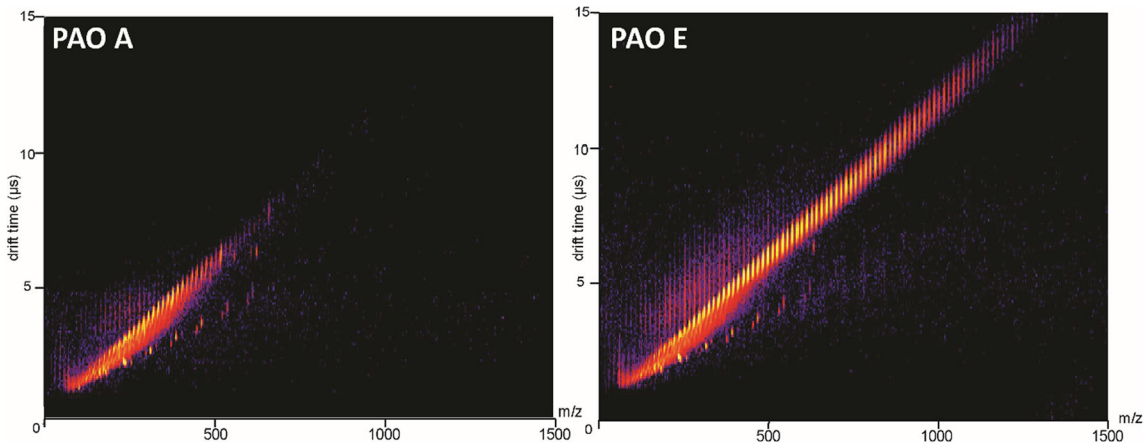

Figure 8. ASAP-IMS-MS 2D drift time versus *m/z* plots for two PAOs, PAO-A (grade 3.6) and PAO-E (grade 150)

be produced from a mixture, more likely of 1-octene and 1-dodecene, as previously proposed for PAO-F.

These fragment ion patterns, specific for each high-grade PAO, can be a useful tool to rapidly differentiate high-grade PAOs and can provide information about the linear alphaolefin used to manufacture the PAO.

The IMS-MS data can provide another possibility to differentiate these PAOs by building two-dimensional "drift time versus *m/z*" plots (Figure 7), as previously shown for polyolefins [23].

The drift time versus *m/z* plot (Figure 7) shows several distributions of ions for each PAO type with a mass shift of 14.02 *m/z* units. These series correspond to the pyrolysis fragment ions of the PAOs. They show narrow distributions for PAO-E (red square) and PAO-F (blue circle), while they are extended for PAO-G which gives a higher amount of pyrolysis fragment ions (yellow triangle**)**. The ion series detected for PAO-E and PAO-F exhibit similar drift time values which were always higher than the drift times of PAO-G ion series. These results indicate that PAO-E and PAO-F ions present more expanded conformations in gas phase than PAO-G. The more compact conformations of PAO-G species are consistent with the presence of more branched molecules. Then, PAO-G yields, in addition to the ion series at high drift time, series of more compact structures (lower drift time) showing higher number of unsaturations according to their molecular formula. As shown, previously, ion CCS decreases as the number of unsaturation increases [54]. It is likely that these very compact ion series specifically detected with PAO-G are produced from more advanced pyrolysis processes [23] which are favored with this highly branched PAO produced by Lewis acid catalysis.

Differentiation Between Low- and High-Grade PAOs The comparison between two dimensional drift time versus *m/z* plots obtained from a high-grade PAO (PAO E, grade 150) and from a low-grade PAO (PAO A, grade 3.6) highlights the difference between light and heavy polyalphaolefins (Figure 8). The IMS-MS 2D plot from PAO E is more complex than that from PAO A because PAO E presents numerous high molecular weight species and different ion series, as expect from a high-viscosity PAO grade. These fingerprints can be used to rapidly identify the synthetic base oils in a formulated lubricant.

Conclusion

The study of low and high PAO grades using ASAP-IMS-MS provides several levels of information. First, we show that tunings of ASAP parameters, in particular, sampling cone voltage and desolvation gas temperature, have an important role and permit to control the ionization processes and the fragmentation patterns. For low PAO grades, three ionization pathways were evidenced: the hydride abstraction $[M-H]^+$, nitrogen insertion $[M+N]^+$, and the formation of $[M-2H]^{+\bullet}$ ions. The relative abundance of each category of ions depends on the cone voltage and desolvation gas temperature, as previously mentioned. At low sampling cone voltage (20 V) and temperatures (< 300°), $[M-H]^+$ ion of the expected PAO according to the supplier data (i.e., C30) as well as pyrolytic fragment ions were detected. Increasing the desolvation gas temperature (> 300 °C) promotes the $[M-2H]^{+\bullet}$ formation and permit to detect higher molecular weight species, while increasing sampling cone voltage (> 40 V) promotes the nitrogen insertion giving $[M+N]^+$ ions. However, at highest desolvation gas temperatures, pyrolytic fragmentation becomes very important and can limit structural investigation. In the case of high PAO grades, even if none of the intact species could be detected, the ASAP mass spectra can however provide information about the repeating unit using the mass shift observed between two adjacent fragment ions of one series and therefore about the linear alphaolefin used to manufacture the PAO. IMS-MS data permit to differentiate low from high grades and/or compact (ramified) from more linear PAO structures using "drift time versus *m/z*" plots. It is also possible to differentiate PAO having low amount of isomers from PAO presenting several isomers with the FWHM of the ion mobility peaks.

Thus, ASAP-IMS-MS appears to be helpful to rapidly identify different grades of PAO, their structural properties (compact conformation or not), and the presence of isomers. All these parameters are particularly important since they could be correlated with the properties and performance of synthetic oils.

Acknowledgements

The authors thank the European Regional Development Fund (ERDF; No. 31708), the Region Normandie (Crunch Network, No. 20-13), the Labex SynOrg (ANR-11-LABX-0029), and TOTAL for the financial support.

References

1. Shubkin, R.L.: In: Lappin, G.R., Sauer, J.D. (eds.) Alphaolefin Application Handbook, pp. 353–373. Marcel Dekker, New York (1989)
2. Rudnick, L.R.: In: Rudnick, L.R. (ed.) Synthetics, Mineral Oils, and Bio-Based Lubricants: Chemistry and Technology, 2nd edn, pp. 3–40. CRC Press, New York (2013)
3. Brown, M., Fotheringham, J.D., Hoyes, T.J., Mortier, R.M., Orszulik, S.T., Randles, S.J., Stroud, P.M.: Synthetic base fluids. In: Mortier, K.A., Fox, M.F., Orszulik, S.T. (eds.) Chemistry and technology of lubricants, pp. 35–74. Springer, Netherlands (2009)
4. Ray, S., Rao, P.V.C., Choudary, N.V.: Poly-α-olefin-based synthetic lubricants: a short review on various synthetic routes. Lubr. Sci. **24**, 23–44 (2012)
5. Mortier, R.M., Fox, M.F., Orszulik, S.T.: Chem Technol Lubricants. (2010). https://doi.org/10.1007/978-1-4020-8662-5
6. Dimaio, A.-J.: Crompton Corp, USA p. 17 (2003)
7. Miyake, S., Kibino, N., Monoi, T., Ohira, H., Inazawa, S.; Showa Denko K. K., Japan: 1993, p 29 pp.
8. Welton, T.: Ionic liquids in catalysis. Coord. Chem. Rev. **248**, 2459–2477 (2004)
9. O'Connor, C.T., Kojima, M.: Alkene oligomerization. Catal. Today. **6**, 329–349 (1990)
10. Shubkin, R.L., Baylerian, M.S., Maler, A.R.: Olefin oligomer synthetic lubricants: structure and mechanism of formation. Ind. Eng. Chem. Prod. Res. Dev. **19**, 15–19 (1980)
11. Wahner, U.M., Brüll, R., Pasch, H., Raubenheimer, H.G., Sanderson, R.: Oligomerisation of 1-pentene with metallocene catalysts. Die Angewandte Makromolekulare Chemie. **270**, 49–55 (1999)
12. Benda, R., Bullen, J., Plomer, A.: Synthetics basics: Polyalphaolefins — base fluids for high-performance lubricants. J. Synthetic Lubric. **13**, 41–57 (1996)
13. Ghosh, R., Bandyopadhyay, A.R., Jasra, R., Gagjibhai, M.M.: Mechanistic study of the oligomerization of olefins. Ind. Eng. Chem. Res. **53**, 7622–7628 (2014)
14. Kapur, G.S., Sarpal, A.S., Sarin, R., Jain, S.K., Srivastava, S.P., Bhatnagar, A.K.: Detailed characterisation of polyalphaolefins and their branched structures using multi-pulse NMR techniques. J. Synthetic Lubric. **15**, 177–191 (1998)
15. Onopchenko, A., Cupples, B.L., Kresge, A.N.: Boron fluoride-catalyzed oligomerization of alkenes: structures, mechanisms, and properties. Ind. Eng. Chem. Prod. Res. Dev. **22**, 182–191 (1983)
16. Scheuermann, S.S., Eibl, S., Bartl, P.: Detailed characterisation of isomers present in polyalphaolefin dimer and the effect of isomeric distribution on bulk properties. Lubr. Sci. **23**, 221–232 (2011)
17. Gee, J.C., Small, B.L., Hope, K.D.: Behavior of protonated cyclopropyl intermediates during polyalphaolefin synthesis: mechanism and predicted product distribution. J. Phys. Org. Chem. **25**, 1409–1417 (2012)
18. Huang, Q., Chen, L., Sheng, Y., Ma, L., Fu, Z., Yang, W.: Synthesis and characterization of oligomer from 1-decene catalyzed by AlCl3/TiCl4/SiO2/Et2AlCl. J. Appl. Polym. Sci. 101, 584–590 (2006)
19. McEwen, C.N., McKay, R.G., Larsen, B.S.: Analysis of solids, liquids, and biological tissues using solids probe introduction at atmospheric pressure on commercial LC/MS instruments. Anal. Chem. **77**, 7826–7831 (2005)
20. McEwen, C.N. In *Encyclopedia of Analytical Chemistry*; John Wiley & Sons, Ltd: 2010, https://doi.org/10.1002/9780470027318.a9045
21. Barrere, C., Maire, F., Afonso, C., Giusti, P.: Atmospheric solid analysis probe-ion mobility mass spectrometry of polypropylene. Anal. Chem. **84**, 9349–9354 (2012)
22. Barrere, C., Hubert-Roux, M., Afonso, C., Racaud, A.: Rapid analysis of lubricants by atmospheric solid analysis probe-ion mobility mass spectrometry. J. Mass Spectrom. **49**, 709–715 (2014)
23. Farenc, M., Witt, M., Craven, K., Barrere-Mangote, C., Afonso, C., Giusti, P.: Characterization of polyolefin pyrolysis species produced under ambient conditions by Fourier transform ion cyclotron resonance mass spectrometry and ion mobility-mass spectrometry. J. Am. Soc. Mass Spectrom. **28**, 507–514 (2017)
24. Twohig, M., Shockcor, J.P., Wilson, I.D., Nicholson, J.K., Plumb, R.S.: Use of an atmospheric solids analysis probe (ASAP) for high throughput screening of biological fluids: preliminary applications on urine and bile. J. Proteome Res. **9**, 3590–3597 (2010)
25. Petucci, C., Diffendal, J.: Atmospheric solids analysis probe: a rapid ionization technique for small molecule drugs. J. Mass Spectrom. **43**, 1565–1568 (2008)
26. Fussell, R.J., Chan, D., Sharman, M.: An assessment of atmospheric-pressure solids-analysis probes for the detection of chemicals in food. TrAC Trends Anal. Chem. **29**, 1326–1335 (2010)
27. Trimpin, S., Wijerathne, K., McEwen, C.N.: Rapid methods of polymer and polymer additives identification: multi-sample solvent-free MALDI, pyrolysis at atmospheric pressure, and atmospheric solids analysis probe mass spectrometry. Anal. Chim. Acta. **654**, 20–25 (2009)
28. Smith, M.J.P., Cameron, N.R., Mosely, J.A.: Evaluating atmospheric pressure solids analysis probe (ASAP) mass spectrometry for the analysis of low molecular weight synthetic polymers. Analyst. **137**, 4524–4530 (2012)
29. Vieillard, J., Hubert-Roux, M., Brisset, F., Soulignac, C., Fioresi, F., Mofaddel, N., Morin-Grognet, S., Afonso, C., Le Derf, F.: Atmospheric solid analysis probe-ion mobility mass spectrometry: an original approach to characterize grafting on cyclic olefin copolymer surfaces. Langmuir. **31**, 13138–13144 (2015)
30. Ballesteros-Gomez, A., de Boer, J., Leonards, P.E.: Novel analytical methods for flame retardants and plasticizers based on gas chromatography, comprehensive two-dimensional gas chromatography, and direct probe coupled to atmospheric pressure chemical ionization-high resolution time-of-flight-mass spectrometry. Anal. Chem. **85**, 9572–9580 (2013)
31. Wang, S.-Z., Fan, X., Zheng, A.-L., Wang, Y.-G., Dou, Y.-Q., Wei, X.-Y., Zhao, Y.-P., Wang, R.-Y., Zong, Z.-M., Zhao, W.: Evaluation of atmospheric solids analysis probe mass spectrometry for the analysis of coal-related model compounds. *Fuel* **117**. Part A. 556–563 (2014)
32. Wu, C., Qian, K., Walters, C.C., Mennito, A.: Application of atmospheric pressure ionization techniques and tandem mass spectrometry for the characterization of petroleum components. Int. J. Mass Spectrom. **377**, 728–735 (2015)
33. Farenc, M., Corilo, Y.E., Lalli, P.M., Riches, E., Rodgers, R.P., Afonso, C., Giusti, P.: Comparison of atmospheric pressure ionization for the analysis of heavy petroleum fractions with ion mobility-mass spectrometry. Energy Fuel. **30**, 8896–8903 (2016)
34. Ahmed, A., Cho, Y.J., No, M.-h., Koh, J., Tomczyk, N., Giles, K., Yoo, J.S., Kim, S.: Application of the Mason−Schamp equation and ion mobility mass spectrometry to identify structurally related compounds in crude oil. Anal. Chem. **83**, 77–83 (2011)
35. Wesdemiotis, C.: Multidimensional mass spectrometry of synthetic polymers and advanced materials. Angew Chem Int Ed Engl. **56**, 1452–1464 (2017)
36. Trimpin, S., Clemmer, D.E.: Ion mobility spectrometry/mass spectrometry snapshots for assessing the molecular compositions of complex polymeric systems. Anal. Chem. **80**, 9073–9083 (2008)
37. Hill, H.H., Siems, W.F.: St. Louis, R.H.: ion mobility spectrometry. *Anal.* Chem. **62**, 1201A–1209A (1990)
38. Kanu, A.B., Dwivedi, P., Tam, M., Matz, L., Hill, H.H.: Ion mobility–mass spectrometry. J. Mass Spectrom. **43**, 1–22 (2008)
39. Giles, K., Pringle, S.D., Worthington, K.R., Little, D., Wildgoose, J.L., Bateman, R.H.: Applications of a travelling wave-based radio-frequency-only stacked ring ion guide. Rapid Commun. Mass Spectrom. **18**, 2401–2414 (2004)

40. Giles, K., Williams, J.P., Campuzano, I.: Enhancements in travelling wave ion mobility resolution. Rapid Commun. Mass Spectrom. **25**, 1559–1566 (2011)
41. Marotta, E., Paradisi, C.: A mass spectrometry study of alkanes in air plasma at atmospheric pressure. J. Am. Soc. Mass Spectrom. **20**, 697–707 (2009)
42. Borsdorf, H., Nazarov, E.G., Eiceman, G.A.: Atmospheric pressure chemical ionization studies of non-polar isomeric hydrocarbons using ion mobility spectrometry and mass spectrometry with different ionization techniques. J. Am. Soc. Mass Spectrom. **13**, 1078–1087 (2002)
43. Bell, S.E., Ewing, R.G., Eiceman, G.A., Karpas, Z.: Atmospheric pressure chemical ionization of alkanes, alkenes, and cycloalkanes. J. Am. Soc. Mass Spectrom. **5**, 177–185 (1994)
44. Jin, C., Viidanoja, J., Li, M., Zhang, Y., Ikonen, E., Root, A., Romanczyk, M., Manheim, J., Dziekonski, E., Kenttämaa, H.I.: Comparison of atmospheric pressure chemical ionization and field ionization mass spectrometry for the analysis of large saturated hydrocarbons. Anal. Chem. **88**, 10592–10598 (2016)
45. Gao, J., Owen, B.C., Borton, D.J., Jin, Z., Kenttämaa, H.I.: HPLC/APCI mass spectrometry of saturated and unsaturated hydrocarbons by using hydrocarbon solvents as the APCI reagent and HPLC mobile phase. J. Am. Soc. Mass Spectrom. **23**, 816–822 (2012)
46. Heine, C.E., Geddes, M.M.: Field-dependent [M – 2H]+. Formation in the field desorption mass spectrometric analysis of hydrocarbon samples. Org. Mass Spectrom. **29**, 277–282 (1994)
47. Li, G., Li, X., Ouyang, Z., Cooks, R.G.: Carbon–carbon bond activation in saturated hydrocarbons by field-assisted nitrogen fixation. Angew. Chem. Int. Ed. **52**, 1040–1043 (2013)
48. Budzikiewicz, H., Djerassi, C., Williams, D.H.: Mass spectrometry of organic compounds. J. Pharm. Sci. **57**, 355–355 (1968)
49. Munson, B. In *Encyclopedia of Analytical Chemistry*; John Wiley & Sons, Ltd: 2006, https://doi.org/10.1002/9780470027318.a6004
50. Field, F.H.: Chemical ionization mass spectrometry. In: Franklin, J.L. (ed.) Ion-molecule reactions: volume 1, pp. 261–313. Springer US: Boston (1972)
51. Field, F.H.: Chemical ionization mass spectrometry. VIII. Alkenes and alkynes. J. Am. Chem. Soc. **90**, 5649–5656 (1968)
52. Harrison: A.G. In: *Chemical Ionization Mass Spectrometry*; 2 Ed.; Taylor & Francis (1992)
53. Farenc, M., Paupy, B., Marceau, S., Riches, E., Afonso, C., Giusti, P.: Effective ion mobility peak width as a new isomeric descriptor for the untargeted analysis of complex mixtures using ion mobility-mass spectrometry. J. Am. Soc. Mass Spectrom. **28**, 2476–2482 (2017)
54. Ponthus, J., Riches, E.: Evaluating the multiple benefits offered by ion mobility-mass spectrometry in oil and petroleum analysis. Int. J. Ion Mobil. Spectrom. **16**, 95–103 (2013)